Hindawi
International Journal of Aerospace Engineering
Volume 2018, Article ID 4083538, 12 pages
https://doi.org/10.1155/2018/4083538

Research Article

Efficient Training Data Generation for Reduced-Order Modeling in a Transonic Flight Regime

Haojie Liu and Yonghui Zhao

State Key Laboratory of Mechanics and Control of Mechanical Structures, Nanjing University of Aeronautics and Astronautics, 210016 Nanjing, China

Correspondence should be addressed to Haojie Liu; liuhj@nuaa.edu.cn

Received 12 March 2018; Revised 3 July 2018; Accepted 30 July 2018; Published 12 September 2018

Academic Editor: Zhiguang SONG

In this study, a time-dependent surrogate approach is presented to generate the training data for identifying the reduced-order model of an unsteady aerodynamic system with the variation of mean angle of attack and Mach number in a transonic flight regime. For such a purpose, a finite set of flight samples are selected to cover the flight range of concern at first. Subsequently, the unsteady aerodynamic outputs of the system under given inputs of filtered white Gaussian noise at these flight samples are simulated via CFD technique which solves Euler equations. The unsteady aerodynamic outputs, which are viewed as a time-dependent function of flight parameters, can be approximated via the Kriging technique at each time step. By this way, the training data for any combination of flight parameters in the range of concern can be obtained without performing any further CFD simulations. To illustrate the accuracy and validity of the training data generated via the proposed approach, the constructed data are used to identify the reduced-order aerodynamic models of a NACA 64A010 airfoil via a robust subspace identification algorithm. The unsteady aerodynamics and aeroelastic responses under various flight conditions in a transonic flight regime are computed. The results agree well with those obtained by using the training data of CFD technique.

1. Introduction

The techniques of computational fluid dynamics (CFD) have been widely used to simulate both linear and nonlinear flow fields for various flight vehicles. However, it is still time-consuming for any high-fidelity CFD techniques to simulate the unsteady aerodynamic loads due to the broad variation of parameters, such as different combinations of mean angle of attack and Mach number. For example, the linear doublet-lattice method has been frequently used for the aeroelastic analysis of aircraft although CFD techniques offer more accurate numerical simulations. In a transonic flight regime, however, the double-lattice method does not work properly because of the aerodynamic nonlinearities coming from shock waves and flow separations [1]. Thus, various CFD-based reduced-order models (ROMs) have been developed [2] so as to provide an effective way to simulate unsteady aerodynamic loads with a high level of accuracy.

In general, the unsteady aerodynamic ROMs can be classified into frequency-domain type and time-domain type. The frequency-domain ROMs mainly contain the proper orthogonal decomposition (POD) approach [3], balanced POD [4], and the harmonic balance approach [5]. On the other hand, the time-domain ROMs include the Eigensystem realization algorithm (ERA) [6], the Volterra theory [7], the auto regressive-moving-average (ARMA) model [8], surrogate models via artificial neural networks [9–11] and Kriging technique [12], and the Wiener-type cascade model [13].

Although a significant progress has been made for the unsteady aerodynamic ROMs, almost all aforementioned ROMs are only valid for a set of fixed flight parameters. It is still time-consuming to generate the unsteady aerodynamic ROMs for a range of flight parameters since the same procedure of computation has to be repeated under each flight condition in the range of concern. Recently, several

reduced-order modeling approaches have been proposed to predict unsteady aerodynamic loads for a range of flight parameters. For example, a surrogate-based recurrence framework ROM was developed to model the unsteady aerodynamics on a rotating airfoil [14]. Yet, it is time-consuming to generate the training data for each combination of parameters in the parameter space. A ROM adaptation approach based on the interpolation in a tangent space to a Grassmann manifold was proposed to predict the aeroelastic characteristics for an F-16 configuration [15]. To obtain new basis vectors for a new flight condition via interpolation, the size of the basis vectors of different local ROMs should be the same so that the accuracy of the POD approach may be decreased. A ROM approach by combining linear convolution with a nonlinear correction factor was proposed to model the aerodynamic characteristics for multiple Mach regimes [16]. However, the approach gives a distinct phase shift at higher oscillation frequencies. A time-dependent surrogate model to fit the relationship between flight parameters and step functions was proposed to model the unsteady and nonlinear aerodynamic loads [17]. Only one kind of input, the pitching motion of the aircraft in their study, can be taken into account at each time. A Kriging surrogate model was proposed to model the unsteady aerodynamic forces with respect to a range of Mach numbers [18]. However, the computational cost for Kriging model increased significantly in order to take the Mach number into consideration. Recently, a reduced-order modeling approach based on recurrent local linear neuro-fuzzy models was developed to model the generalized aerodynamic forces over a range of Mach numbers [19]. To guarantee the accuracy of the local linear neuro-fuzzy model, the flight parameters for training data should be selected carefully in the flight range of concern. Very recently, a nonlinear interpolation method based on a set of local linear state-space models was proposed to model the generalized aerodynamic forces for an elastic wing with control surfaces [20]. Nevertheless, enough local linear state-space models were required to cover the flight range of concern and only Mach number variations were taken into consideration.

Almost all aforementioned unsteady aerodynamic ROMs, which take flight parameter variations into account, require enough training data to capture the dynamic characteristics of the unsteady aerodynamic systems. However, it is time-consuming to generate the training data via any direct CFD simulations when both Mach number and mean angle of attack are taken into consideration. The motivation of this study is to generate the training data efficiently for a range of flight parameters including mean angle of attack and Mach number in a transonic flight regime. For such a purpose, a time-dependent surrogate approach is proposed. Once the Kriging models are constructed via the proposed approach, the training data under an arbitrary flight condition in the range of concern can be obtained without performing any further CFD simulations. The remainder of the paper is organized as follows. In Section 2, the theoretical background of the training data generation approach and the robust subspace algorithm is presented. In Section 3, the unsteady aerodynamics and aeroelastic responses of a NACA 64A010 airfoil under different flight conditions in a transonic flight regime are investigated to validate the proposed approach. In Section 4, some conclusions are given.

2. Theoretical Background

In this section, the theoretical background of the training data generation approach and the robust subspace algorithm is presented. The flowchart of the reduced-order modeling approach is shown in Figure 1. The first step is to obtain the unsteady aerodynamic outputs of the system via direct CFD simulations at a finite set of flight samples selected to cover the flight range of concern. Then, a time-dependent surrogate method based on the Kriging technique is used to approximate the relationship between the unsteady aerodynamic outputs of the system and the flight parameters. Afterwards, with the training data obtained, the robust subspace algorithm is implemented to identify the discrete-time state-space model under an arbitrary flight condition.

2.1. Selection of Excitation Signal. As well known, the dynamic characteristics of an unsteady aerodynamic system of concern should be appropriately excited via the input signal in order to construct the training data for successfully identifying the corresponding time-domain ROMs. For this purpose, the filtered white Gaussian noise (FWGN) is used as the input signal to make CFD simulations. Under such a type of excitation, only the frequency response spectrum of concern can be excited and there is no need to repeat computations for each combination of frequency and amplitude.

Once the type of input signal is determined, it is necessary to select the sampling rate and the sampling length for the input signal. The sampling rate f_S determined by the time step Δt of the CFD solver is given as follows:

$$f_S = \frac{1}{\Delta t}. \tag{1}$$

According to the Nyquist sampling theorem, the Nyquist frequency f_N is $f_S/2$ which must exceed the maximal frequency of concern. Furthermore, the frequency resolution of the input signal with the sampling length N, given by f_N/N, should be adequate for the representation of the minimal frequency of concern. Hence, the time step Δt and the sampling length N for the input signal need to be adjusted carefully.

Although only one unsteady aerodynamic simulation under FWGN excitation is required under each flight condition, it is still time-consuming to generate the training data to capture the dynamic characteristics of an unsteady aerodynamic system in the mean angle of attack and Mach number space.

2.2. Time-Dependent Surrogate Approach for Training Data Generation. To generate the training data for a range of flight parameters efficiently, a time-dependent surrogate method based on the Kriging technique is proposed in this subsection. Similar to the previous study [17], the unsteady aerodynamic outputs of the system under the FWGN excitation and

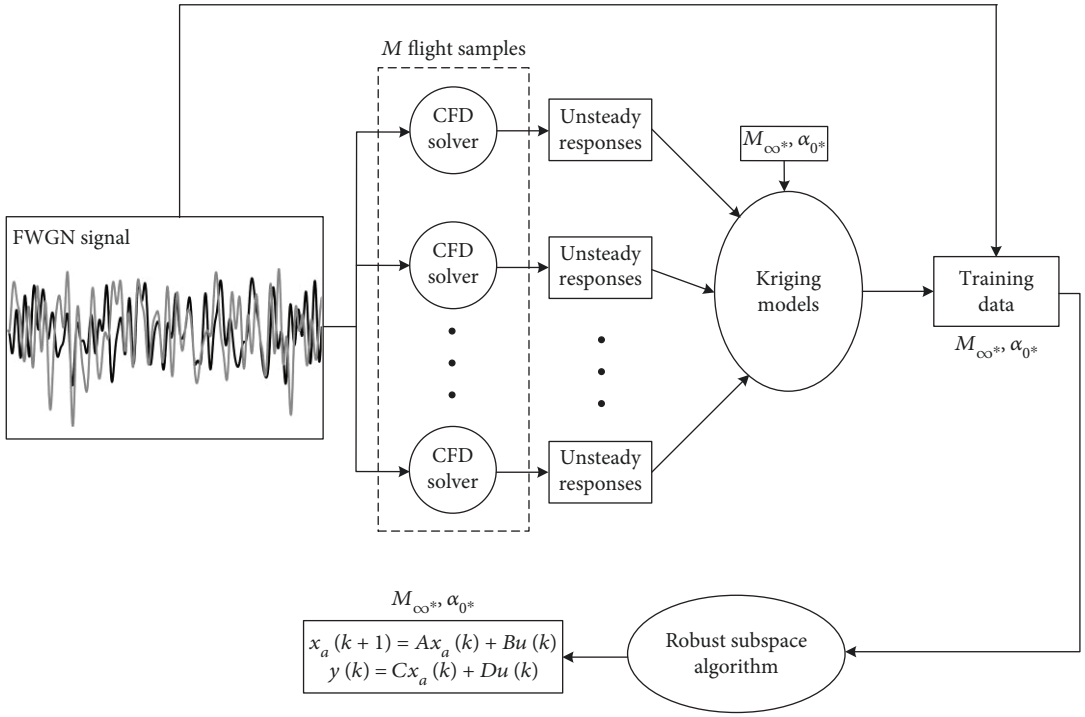

Figure 1: The flowchart of the reduced-order modeling approach.

a finite set of flight conditions are considered as a set of time-correlated spatial processes. Under such an assumption, the surrogate techniques can be used to model the time-dependent outputs of the aerodynamic system at each time step as a function of flight parameters. Here, the Kriging technique is implemented since it has good accuracy and robustness with small data sets [21].

To approximate the input-output relationship between the flight parameters and the unsteady aerodynamic outputs of the system, M flight samples need to be selected to cover the range of concern at first. The design of experimental studies [22] can be used to select these samples from the mean angle of attack α_0 and Mach number M_∞ space. It is worthy to note that the selection of the input parameters strongly depends on the flight regime of concern and the aircraft configuration. For example, more flight parameter samples need to be placed at the region where there exist strong aerodynamic nonlinearities in the flow field. Subsequently, the input vector $\mathbf{X}$ for the Kriging technique can be defined as

$$\mathbf{X} = \begin{bmatrix} M_{\infty,1} & \alpha_{0,1} \\ M_{\infty,2} & \alpha_{0,2} \\ \vdots & \vdots \\ M_{\infty,M} & \alpha_{0,M} \end{bmatrix}. \tag{2}$$

Under each flight condition defined by $M_{\infty,i}$ and $\alpha_{0,i}$, an unsteady aerodynamic computation needs to be performed via direct CFD simulation under the given FWGN excitation. The corresponding outputs of the aerodynamic system of the M flight samples can be written as

$$\mathbf{Y}_o = \begin{bmatrix} \mathbf{y}_{1,1} & \mathbf{y}_{2,1} & \cdots & \mathbf{y}_{N,1} \\ \mathbf{y}_{1,2} & \mathbf{y}_{2,2} & \cdots & \mathbf{y}_{N,2} \\ \vdots & \vdots & \ddots & \vdots \\ \mathbf{y}_{1,M} & \mathbf{y}_{2,M} & \cdots & \mathbf{y}_{N,M} \end{bmatrix}, \tag{3}$$

where $\mathbf{y}_{i,j}$ is the aerodynamic output vector and N is the number of time steps of the FWGN excitation. With the input vector $\mathbf{X}$ and the output vector $\mathbf{Y}_o$ known, the Kriging technique can be used to approximate the relationship between the flight parameter and the aerodynamic outputs of the system at each time step.

What follows is a brief description of the Kriging technique, where the Kriging model approximates the target function at an untried site $\mathbf{x}_*$ as

$$\Phi(\mathbf{x}_*) = \mathbf{f}(\mathbf{x}_*)\boldsymbol{\beta} + z(\mathbf{x}_*), \tag{4}$$

Here, $\mathbf{f}(\mathbf{x}_*)$ and $\boldsymbol{\beta}$ are the regression model and the regression coefficients, respectively. In (4), the first term is the mean value, which can be thought as a globally valid trend function. The second term $z(\mathbf{x}_*)$ given in (4) is a Gaussian distributed error term with zero mean and variance σ^2. To construct the Kriging model, the values of the regression coefficients $\boldsymbol{\beta}$ can be approximated by solving a least-

square regression problem as follows:

$$\widehat{\boldsymbol{\beta}} = \left(\mathbf{F}^{\mathrm{T}}\left(\mathbf{R}^{-1}\right)\mathbf{F}\right)^{-1}\mathbf{F}^{\mathrm{T}}\mathbf{R}^{-1}\mathbf{h}, \tag{5}$$

where $\mathbf{R}$ is the spatial correlation matrix. $\mathbf{h}$ and $\mathbf{F}$ are the $M \times 1$ output vector and the $M \times M$ mapping matrix at the sample inputs, respectively. $\mathbf{h}$ and $\mathbf{F}$ are defined as

$$\mathbf{h} = \begin{bmatrix} y_1 \\ y_2 \\ \vdots \\ y_M \end{bmatrix},$$
$$\mathbf{F} = \begin{bmatrix} f_1(\mathbf{x}_1) & f_2(\mathbf{x}_1) & \cdots & f_{r+1}(\mathbf{x}_1) \\ f_1(\mathbf{x}_2) & f_2(\mathbf{x}_2) & \cdots & f_{r+1}(\mathbf{x}_2) \\ \vdots & \vdots & \ddots & \vdots \\ f_1(\mathbf{x}_M) & f_2(\mathbf{x}_M) & \cdots & f_{r+1}(\mathbf{x}_M) \end{bmatrix}. \tag{6}$$

With the vector $\mathbf{r} = [R(\mathbf{x}_*, \mathbf{x}_1)R(\mathbf{x}_*, \mathbf{x}_2) \cdots R(\mathbf{x}_*, \mathbf{x}_M)]^{\mathrm{T}}$, the prediction at an unsampled location $\mathbf{x}_*$ can be obtained as

$$\widehat{\Phi}(\mathbf{x}_*) = \mathbf{f}(\mathbf{x}_*)\widehat{\boldsymbol{\beta}} + \mathbf{r}^{\mathrm{T}}\mathbf{R}^{-1}\left(\mathbf{h} - \mathbf{F}\widehat{\boldsymbol{\beta}}\right). \tag{7}$$

It has to be noted that one mapping function $\widehat{\Phi}$ needs to be constructed for each component of the output vector at each time step. Once the Kriging models are constructed, the unsteady aerodynamic outputs of the system under an arbitrary flight condition in the range of concern can be obtained without performing any further CFD simulations. For example, the corresponding aerodynamic outputs of the system under the same FWGN excitation for the mean angle of attack α_{0*} and Mach number $M_{\infty*}$ can be written as

$$\begin{bmatrix} y_{1*} & y_{2*} & \cdots & y_{N*} \end{bmatrix} = \left[\widehat{\Phi}_1(M_{\infty*}, \alpha_{0*})\widehat{\Phi}_2(M_{\infty*}, \alpha_{0*}) \cdots \widehat{\Phi}_N(M_{\infty*}, \alpha_{0*})\right]. \tag{8}$$

Hence, the training data under an arbitrary flight condition in the range of concern can be obtained efficiently via the proposed approach.

2.3. Robust Subspace Algorithm. With the training data obtained via the time-dependent surrogate approach, a time-domain ROM approach can be used to construct the unsteady aerodynamic ROM. In this study, the robust subspace algorithm [23] is implemented to identify the discrete-time state-space models. This algorithm is always numerically stable and convergent and has no identification problems, such as lack of convergence, slow convergence, or numerical instability.

A brief description of the algorithm is given as follows. The discrete-time state-space model assumes the following model structure:

$$\begin{aligned} \mathbf{x}_a(k+1) &= \mathbf{A}\mathbf{x}_a(k) + \mathbf{B}\mathbf{u}(k), \\ \mathbf{y}(k) &= \mathbf{C}\mathbf{x}_a(k) + \mathbf{D}\mathbf{u}(k), \end{aligned} \tag{9}$$

where $\mathbf{x}_a$, $\mathbf{u}$, and $\mathbf{y}$ are the vectors of state, input, and output variables, respectively. Given the training data, four constant matrices $\mathbf{A}$, $\mathbf{B}$, $\mathbf{C}$, and $\mathbf{D}$ are estimated such that the unsteady aerodynamic outputs of the system under the FWGN excitation can be reproduced.

At first, the input and output Hankel block matrices based on the training data are defined as

$$\left(\frac{\mathbf{U}_p}{\mathbf{U}_f}\right) \stackrel{\text{def}}{=} \left(\begin{array}{cccc} \mathbf{u}_0 & \mathbf{u}_1 & \cdots & \mathbf{u}_{j-1} \\ \mathbf{u}_1 & \mathbf{u}_2 & \cdots & \mathbf{u}_j \\ \cdots & \cdots & \cdots & \cdots \\ \mathbf{u}_{i-1} & \mathbf{u}_i & \cdots & \mathbf{u}_{i+j-2} \\ \hline \mathbf{u}_i & \mathbf{u}_{i+1} & \cdots & \mathbf{u}_{i+j-1} \\ \mathbf{u}_{i+1} & \mathbf{u}_{i+2} & \cdots & \mathbf{u}_{i+j} \\ \cdots & \cdots & \cdots & \cdots \\ \mathbf{u}_{2i-1} & \mathbf{u}_{2i} & \cdots & \mathbf{u}_{2i+j-2} \end{array}\right),$$
$$\left(\frac{\mathbf{Y}_p}{\mathbf{Y}_f}\right) \stackrel{\text{def}}{=} \left(\begin{array}{cccc} \mathbf{y}_0 & \mathbf{y}_1 & \cdots & \mathbf{y}_{j-1} \\ \mathbf{y}_1 & \mathbf{y}_2 & \cdots & \mathbf{y}_j \\ \cdots & \cdots & \cdots & \cdots \\ \mathbf{y}_{i-1} & \mathbf{y}_i & \cdots & \mathbf{y}_{i+j-2} \\ \hline \mathbf{y}_i & \mathbf{y}_{i+1} & \cdots & \mathbf{y}_{i+j-1} \\ \mathbf{y}_{i+1} & \mathbf{y}_{i+2} & \cdots & \mathbf{y}_{i+j} \\ \cdots & \cdots & \cdots & \cdots \\ \mathbf{y}_{2i-1} & \mathbf{y}_{2i} & \cdots & \mathbf{y}_{2i+j-2} \end{array}\right), \tag{10}$$

where the number j of columns is given as

$$j = N - 2i + 1. \tag{11}$$

In (11), N is the length of training data and i is the number of block rows in the Hankel block matrices. Then, based on the RQ decomposition of the Hankel block matrix, the weighted oblique projection $o_i\Pi_{\mathbf{U}_f^\perp}$ can be computed. The singular value decomposition of the weighted oblique projection is given as follows:

$$o_i\Pi_{\mathbf{U}_f^\perp} = \mathbf{U}\mathbf{S}\mathbf{V}^T. \tag{12}$$

The order of state-space model can be determined by inspecting the singular values in $\mathbf{S}$. Afterwards, $\mathbf{U}_1$ and

$\mathbf{S}_1$ can be obtained according to the order and the matrices. The extended observability matrix Γ_i can be computed as

$$\Gamma_i = \mathbf{U}_1 \mathbf{S}_1^{1/2}. \tag{13}$$

Here, Γ_{i-1} denotes the matrix Γ_i without the last p rows. To this end, the system matrices **A**, **B**, **C**, and **D** can be obtained with the matrices Γ_i, Γ_{i-1}, and the decomposition matrix of the Hankel block matrix. For further details, one can refer [23].

In summary, the efficiency of the algorithm enables one to identify the unsteady aerodynamic ROM quickly under an arbitrary flight condition.

3. Case Studies

This section presents the study on the unsteady aerodynamic problem and aeroelastic problem of a NACA 64A010 airfoil, respectively, for the mean angle of attack α_0 ranging from 0 to 5 deg and the Mach number M_∞ ranging from 0.75 to 0.85 so as to validate the proposed approach.

The airfoil of concern has two degrees of freedom, as shown in Figure 2, where $\bar{x}_\alpha$ is the dimensionless distance between the center of gravity and the stiffness center, $\bar{r}_\alpha$ is the gyration radius of the airfoil around the stiffness center, ω_α and ω_h are the uncoupled natural frequencies of the pitch and plunge, and b, μ, V_∞, and V_∞^* are the half-chord length, mass ratio, free-stream velocity, and dimensionless velocity, respectively. With the dimensionless time $\tau = \omega_\alpha \cdot t$, the dynamic equation of the airfoil can be established in the following state-space form.

$$\dot{\mathbf{x}} = \mathbf{A}_s \cdot \mathbf{x} + \mathbf{B}_s \cdot \mathbf{f}_a(\mathbf{x}, t). \tag{14}$$

The vectors and matrices in (14) can be written as

$$\begin{aligned}
\mathbf{A}_s &= \begin{bmatrix} \mathbf{0}_{2\times 2} & \mathbf{I}_{2\times 2} \\ -\mathbf{M}^{-1}\mathbf{K} & \mathbf{0}_{2\times 2} \end{bmatrix}, \\
\mathbf{B}_s &= \begin{bmatrix} \mathbf{0}_{2\times 2} \\ \mathbf{M}^{-1} \end{bmatrix}, \\
\mathbf{f}_a &= \frac{(V_\infty^*)^2}{\pi} \begin{Bmatrix} -C_l \\ 2C_m \end{Bmatrix}, \\
\boldsymbol{\xi} &= \begin{Bmatrix} \dfrac{h}{b} \\ \alpha \end{Bmatrix}, \\
\mathbf{x} &= \begin{Bmatrix} \boldsymbol{\xi} \\ \dot{\boldsymbol{\xi}} \end{Bmatrix},
\end{aligned} \tag{15}$$

where the mass and stiffness matrices are defined as

$$\begin{aligned}
\mathbf{M} &= \begin{bmatrix} 1 & \bar{x}_\alpha \\ \bar{x}_\alpha & \bar{r}_\alpha^2 \end{bmatrix}, \\
\mathbf{K} &= \begin{bmatrix} \left(\dfrac{\omega_h}{\omega_\alpha}\right)^2 & 0 \\ 0 & \bar{r}_\alpha^2 \end{bmatrix}.
\end{aligned} \tag{16}$$

The structural parameters of the airfoil are chosen to be $\bar{x}_\alpha = 1.8$, $\bar{r}_\alpha^2 = 3.48$, $\bar{a} = -2.0$, $\omega_h = 100$ rad/sec, $\omega_\alpha = 100$ rad/sec, and $\mu = 60$, respectively.

3.1. Training Data for the Unsteady Aerodynamic System. The CFD technique which solves the Euler equations [13, 18] is used to compute the unsteady aerodynamics over the airfoil in transonic regime. The spatial discretization of the CFD solver is based on the cell-centered finite-volume approach. The widely used central scheme with artificial dissipation is employed for convective flux calculation. The dual time-stepping approach is employed for unsteady simulations. After performing mesh and time step sensitivity analyses, the unstructured mesh with 4098 cells and dimensionless fluid time step 0.2 are used in the present study. Figure 3 presents the CFD grid consisting of 4098 triangle elements and 2145 nodes. The high-fidelity CFD solver needs to be validated at first. In order to validate the Euler solver used in the present study, the test case CT6 of [24] is studied. For such case, the free stream Mach number is 0.796 and the 64A010 airfoil pitches around its quarter-chord point and the pitching motion are governed as

$$\alpha(t) = \alpha_0 + \alpha_A \sin(\omega t), \tag{17}$$

where $\alpha_0 = 0$ deg and $\alpha_A = 1.01$ deg are the mean angle of attack and the amplitude of pitching oscillation, respectively. The relationship between the angular frequency ω and the reduced frequency $k_r = 0.202$ is described as

$$k_r = \frac{\omega c}{2V_\infty}, \tag{18}$$

where c and V_∞ are the chord length and the free-stream velocity, respectively. As shown in Figure 4, the CFD lift coefficients agree well with the experimental data. However, there are apparent differences for the moment coefficients between the numerical and experimental results. Such discrepancy may be due to the high sensitivity of the moment coefficients to the location of shock wave.

In the numerical simulations, the dimensionless bandwidth of the FWGN excitation signal is chosen to be 0.01~0.4. Figure 5 presents the time histories of the two FWGN excitation signals selected to drive the pitch and plunge motions of the airfoil, respectively. The length of the input signal in CFD simulations is taken as 2000. Subsequently, 20 flight samples are selected for the mean angle of attack α_0 in [0, 5] deg and for the Mach number M_∞ in [0.75, 0.85], respectively, as shown in Figure 6. For each flight

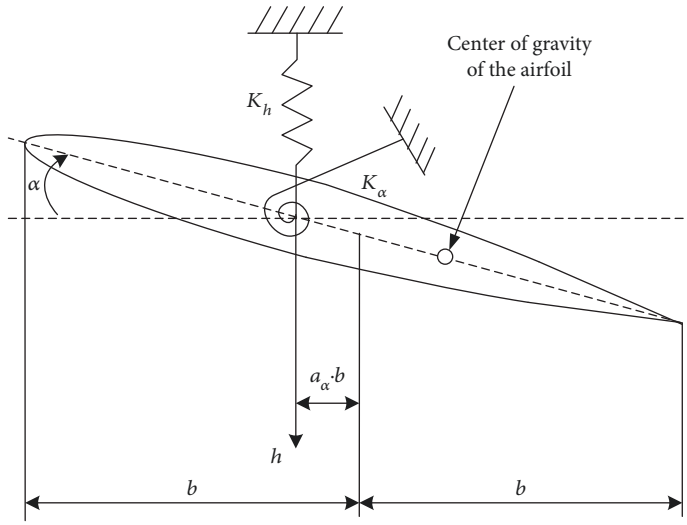

Figure 2: An airfoil of two degrees of freedom.

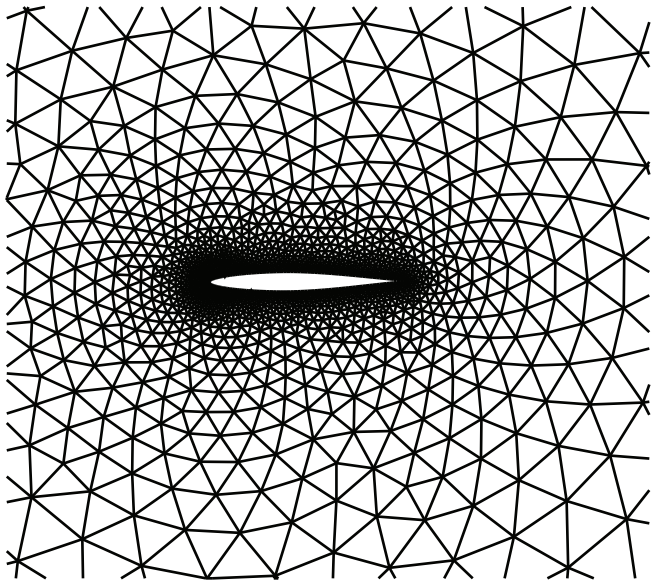

Figure 3: The CFD grid for the NACA64A010 airfoil.

parameter sample, an unsteady aerodynamic simulation is performed via the CFD solver.

According to the time-dependent surrogate approach, 4000 Kriging models are required since the length of the FWGN excitation is 2000 for two unsteady aerodynamic outputs of the system, that is, the lift coefficient C_l and the moment coefficient C_m. To demonstrate the accuracy of the training data, C_l and C_m are predicted via the Kriging models under two flight conditions in a transonic flight regime, one with $M_\infty = 0.76$ and $\alpha_0 = 1$ deg and the other with $M_\infty = 0.82$ and $\alpha_0 = 4$ deg. As shown in Figures 7 and 8, the results predicted via the Kriging models agree well with those obtained via the direct CFD technique.

The CPU time to construct the Kriging models is shown in Table 1, where all the computations are performed by using a laptop with two CPUs of 2.4 GHz. Even though the total CPU time cost associated with the construction of the Kriging models is a little bit expensive, the training data under an arbitrary flight condition in the range of concern can be obtained efficiently without performing any further CFD simulation. For example, the computational time of the direct CFD approach which solves Euler equations is about 0.284 h in order to obtain the training data at $M_\infty = 0.76$ and $\alpha_0 = 3$ deg, while the computational time of the Kriging models for the same case is 0.006 h only.

3.2. Unsteady Aerodynamic Prediction. To demonstrate the application of the training data in unsteady aerodynamic prediction, the constructed data are used to identify the state-space models via the robust subspace algorithm. The

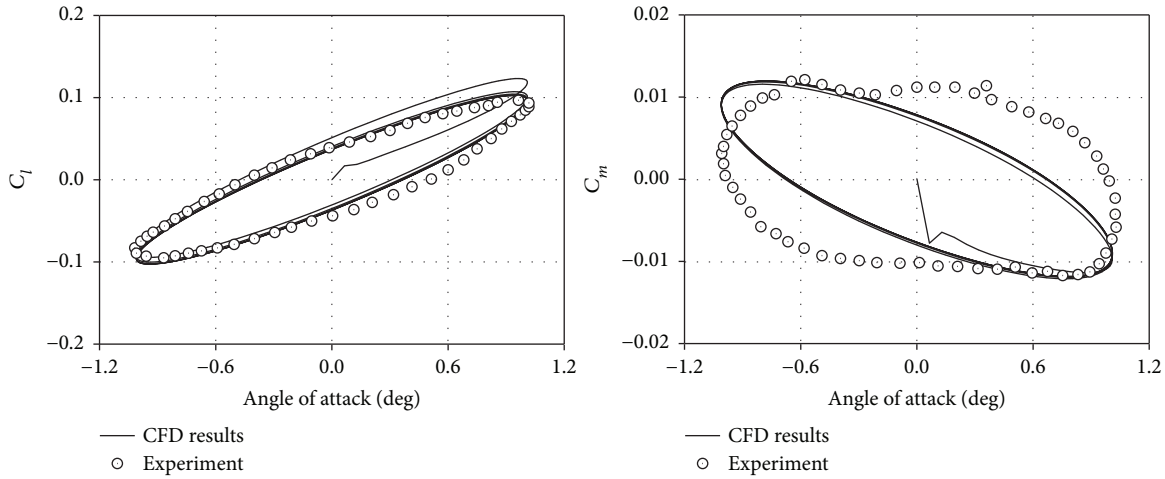

Figure 4: Lift and moment coefficient loops for a NACA 64A010 airfoil at Mach number 0.796.

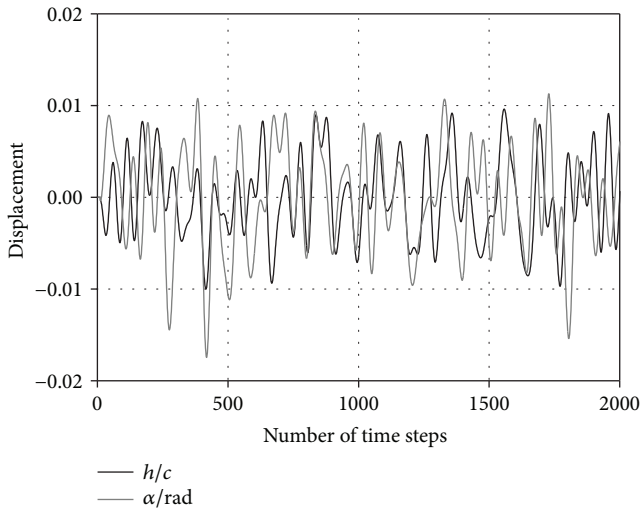

Figure 5: The FWGN excitation signals to drive pitch and plunge motions.

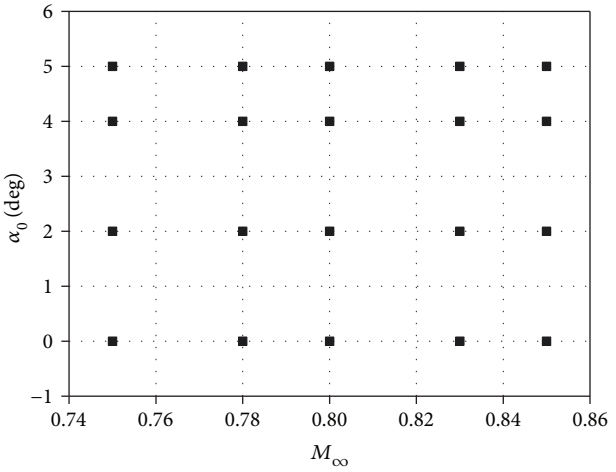

Figure 6: The flight parameter samples to cover the range of concern.

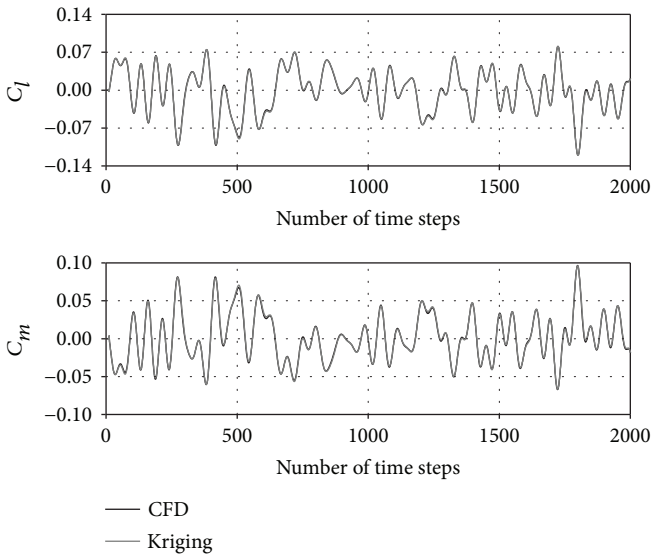

Figure 7: The training data validation of a NACA 64A010 airfoil at $M_\infty = 0.76$ and $\alpha_0 = 1$ deg.

unsteady aerodynamic outputs of the system are computed under different excitation signals, and the results are compared with those obtained by using the CFD training data.

At first, the FWGN excitation signals, not the same as the training signal during the ROM construction, are used to drive the airfoil at $M_\infty = 0.76$ and $\alpha_0 = 3$ deg. The pitch and plunge motions of the airfoil are shown in Figure 9. The corresponding unsteady aerodynamic coefficients are shown in Figure 10. For further comparison, the flight condition with $M_\infty = 0.82$ and $\alpha_0 = 5$ deg is also selected. The excitation signals and the corresponding unsteady aerodynamic results are presented in Figures 11 and 12, respectively. In addition, a harmonic oscillation is chosen as the input signal at $M_\infty = 0.84$ and $\alpha_0 = 0$ deg. The unsteady aerodynamic results are presented in Figure 12.

As can be seen from Figures 10, 12, and 13, the time histories of C_l and C_m obtained via the ROM2s identified

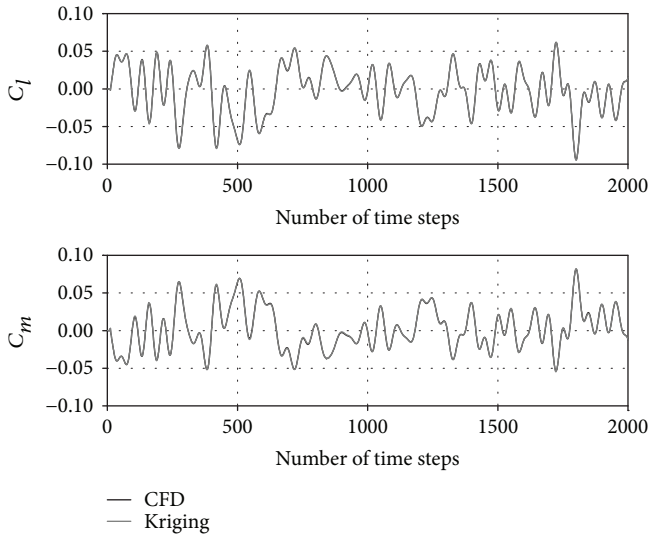

Figure 8: The training data validation of a NACA 64A010 airfoil at $M_\infty = 0.82$ and $\alpha_0 = 4$ deg.

Table 1: The computational cost associated with the time-dependent surrogate approach.

	CPU time
Computation of the 20 training cases	4.98 h
Generation of the Kriging models	0.01 h
Total CPU time	4.99 h

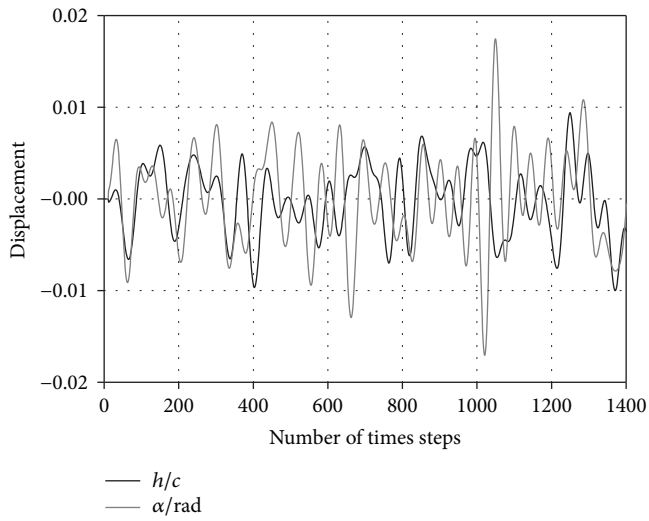

Figure 9: The pitch and plunge motions under the FWGN excitation for ROM validation at $M_\infty = 0.76$ and $\alpha_0 = 3$ deg.

by using the time-dependent surrogate approach agree well with those of ROM1s identified by using the direct CFD simulation data. That is, the proposed approach is able to generate good training data for ROMs in a transonic flight regime.

3.3. Aeroelastic Time-Marching Simulation. To further demonstrate the performance of the proposed approach in the

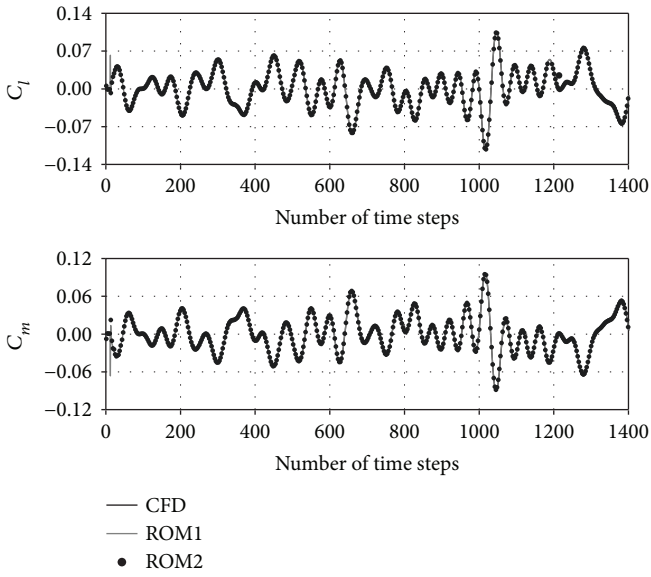

Figure 10: The ROM validation under the FWGN excitation at $M_\infty = 0.76$ and $\alpha_0 = 3$ deg (ROM1-training data via CFD; ROM2-training data via the proposed method).

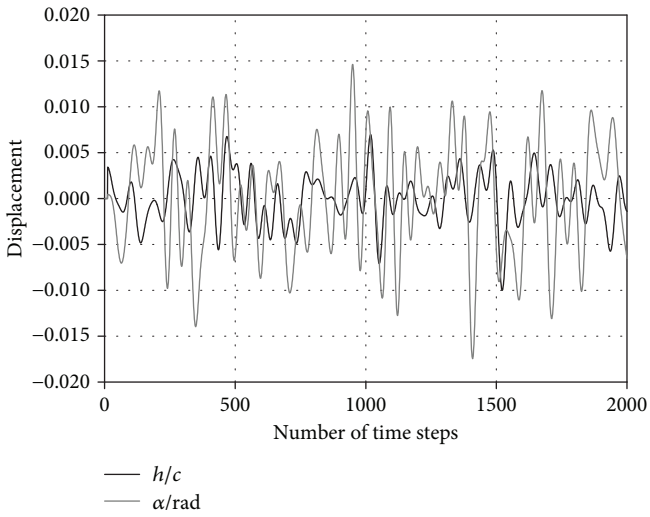

Figure 11: The FWGN excitation signals for ROM validation at $M_\infty = 0.82$ and $\alpha_0 = 5$ deg.

flutter prediction in a transonic flight regime, the ROM2s are coupled with the structural model to make time-marching simulations. At first, the airfoil is forced to make three complete cycles of harmonic motion in pitch at the frequency $\omega_\alpha/2$. Then, the aeroelastic system is allowed to evolve by its own self-induced loads.

In the present case, the aeroelastic responses of the airfoil predicted via the ROM2s and ROM1s are compared under two flight conditions. As shown in Figure 14, the aeroelastic responses of the airfoil with $M_\infty = 0.81$ and $\alpha_0 = 0$ deg are computed for $V^*_\infty = 0.73$. Both ROM2 and ROM1 can predict a neutrally stable oscillation. Afterwards, the aeroelastic responses of the airfoil with $M_\infty =$

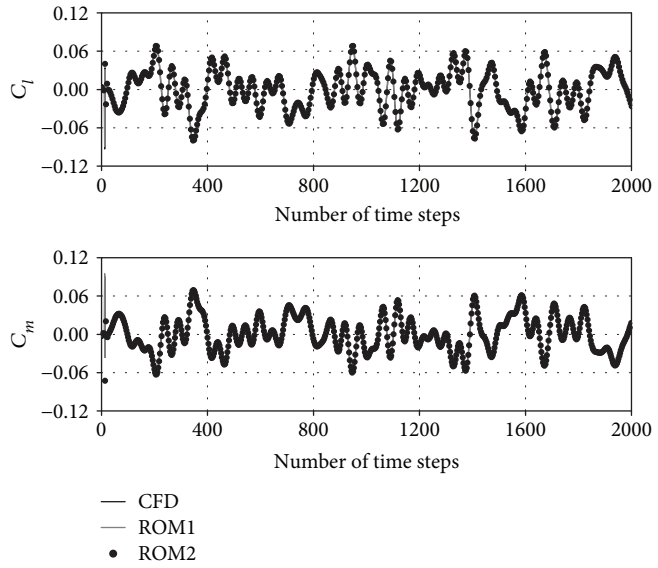

Figure 12: The ROM validation under the FWGN excitation at $M_\infty = 0.82$ and $\alpha_0 = 5$ deg (ROM1-training data via CFD; ROM2-training data via the proposed method).

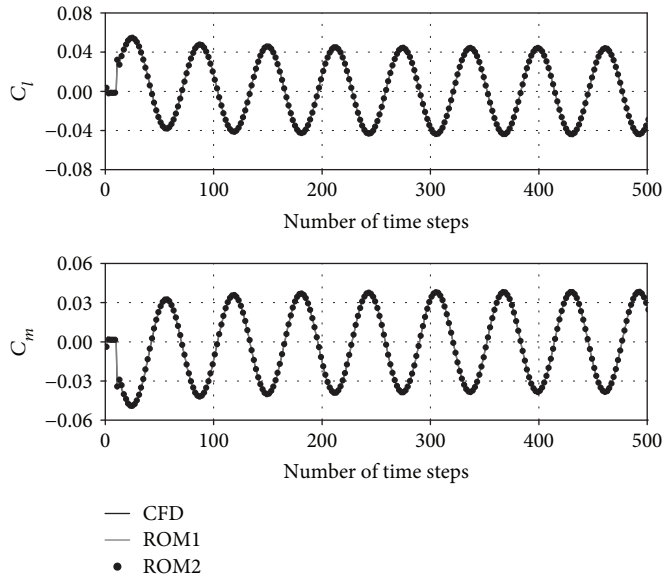

Figure 13: The ROM validation under the harmonic excitation at $M_\infty = 0.84$ and $\alpha_0 = 0$ deg (ROM1-training data via CFD; ROM2-training data via the proposed method).

0.85 and $\alpha_0 = 1$ deg are evaluated. As shown in Figure 15, the results of ROM2 and ROM1 present a neutrally stable oscillation at $V^*_\infty = 0.57$.

Finally, Figures 16 and 17 give the flutter boundaries of the aeroelastic model with the mean angle of attack $\alpha_0 = 1$ deg and $\alpha_0 = 3$ deg, respectively. As shown in these two figures, the computational results based on ROM2s and ROM1s get a good agreement in the flutter boundaries. Nevertheless, the computation of ROM2 is much more efficient than that of ROM1 since no further CFD simulations are required once the Kriging models are constructed.

As can be seen from the flutter boundaries of the airfoil at different mean angle of attack, the aeroelastic characteristics of the model are very sensitive to the mean angle of attack in a transonic flight regime. Hence, the effects of the variations of the mean angle of attack have to be taken into account for aeroelastic analysis.

4. Conclusions

In this study, an efficient approach is proposed to generate the training data for constructing the reduced-order model of an

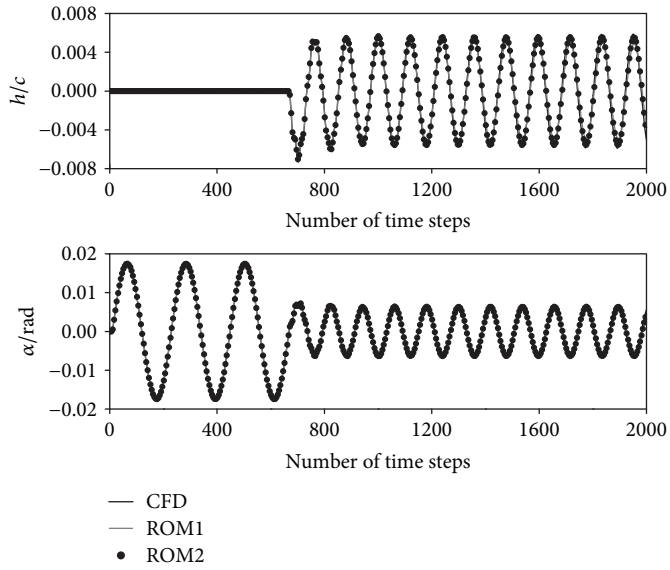

Figure 14: The aeroelastic responses of the airfoil for $V^*_\infty = 0.73$ at $M_\infty = 0.81$ and $\alpha_0 = 0$ deg (ROM1-training data via CFD; ROM2-training data via the proposed method).

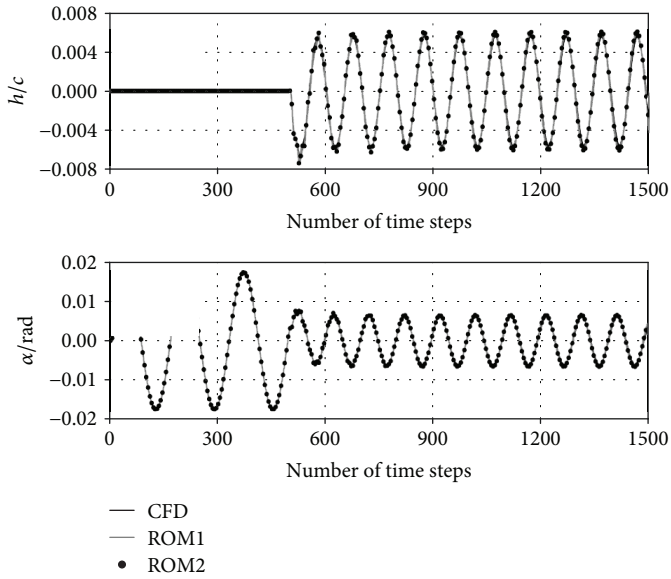

Figure 15: The aeroelastic responses of the airfoil for $V^*_\infty = 0.57$ at $M_\infty = 0.85$ and $\alpha_0 = 1$ deg (ROM1-training data via CFD; ROM2-training data via the proposed method).

unsteady aerodynamic system with the variation of flight parameters in a transonic flight regime. The Kriging technique is used in the approach to approximate the relationship between the unsteady aerodynamic outputs of the system and the flight parameters. No further CFD simulations are required to generate the training data once the Kriging models are constructed. The training data obtained via the proposed approach are used to identify the reduced-order aerodynamic models of a NACA 64A010 airfoil via a robust subspace identification algorithm. The unsteady aerodynamics and aeroelastic responses of the airfoil under various flight conditions in a transonic flight regime are computed. The results agree well with those obtained by using the direct simulations of computational fluid dynamics.

When the time-dependent surrogate approach is applied to a three-dimensional aeroelastic model in a transonic flight regime, it is expected to save more computation time compared with two-dimensional cases. Furthermore, the unsteady aerodynamics generated via the approach can be used as the validation data to determine the validation region of an unsteady aerodynamic ROM. Based on the time-dependent surrogate approach, a method by assembling the

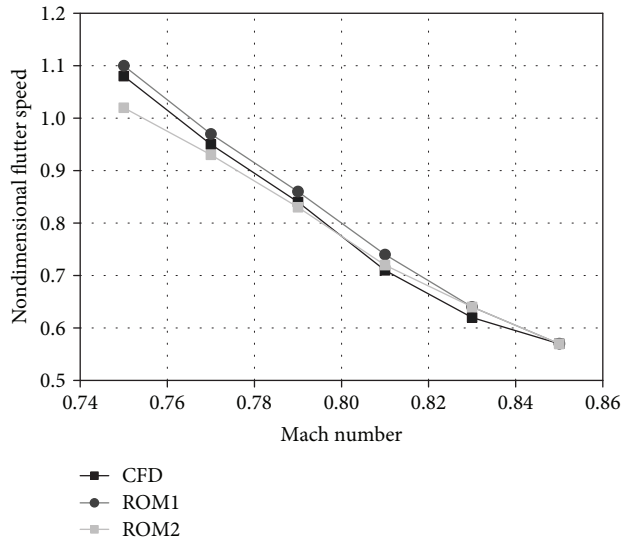

Figure 16: The flutter boundary of the airfoil with the mean angle of attack $\alpha_0 = 1$ deg (ROM1-training data via CFD; ROM2-training data via the proposed method).

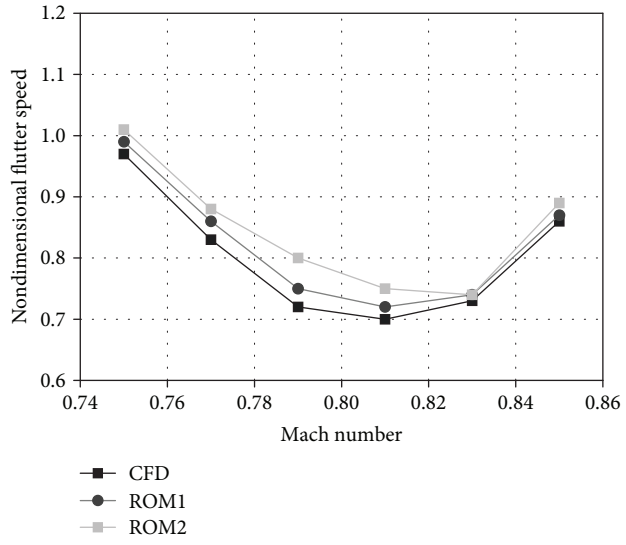

Figure 17: The flutter boundary of the airfoil with the mean angle of attack $\alpha_0 = 3$ deg (ROM1-training data via CFD; ROM2-training data via the proposed method).

aerodynamic outputs of a set of precomputed local linear models will be investigated to construct the aerodynamic ROM for a range of flight parameters.

Data Availability

The data used to support the findings of this study are available from the corresponding author upon request.

Conflicts of Interest

The authors declare that they have no competing interests.

Acknowledgments

This work was supported by the National Natural Science Foundation of China under grant 11472128 and grant 11502106, National Science Foundation of Jiangsu Province under Grant BK20150736, and Aeronautical Science Foundation of China under Grant 2015ZA52004.

References

[1] O. O. Bendiksen, "Review of unsteady transonic aerodynamics: theory and applications," *Progress in Aerospace Sciences*, vol. 47, no. 2, pp. 135–167, 2011.

[2] D. J. Lucia, P. S. Beran, and W. A. Silva, "Reduced-order modeling: new approaches for computational physics," *Progress in Aerospace Sciences*, vol. 40, no. 1-2, pp. 51–117, 2004.

[3] K. C. Hall, J. P. Thomas, and E. H. Dowell, "Proper orthogonal decomposition technique for transonic unsteady aerodynamic flows," *AIAA Journal*, vol. 38, no. 10, pp. 1853–1862, 2000.

[4] C. W. Rowley, "Model reduction for fluids, using balanced proper orthogonal decomposition," *International Journal of Bifurcation and Chaos*, vol. 15, no. 03, pp. 997–1013, 2005.

[5] J. P. Thomas, E. H. Dowell, and K. C. Hall, "Modeling viscous transonic limit cycle oscillation behavior using a harmonic balance approach," *Journal of Aircraft*, vol. 41, no. 6, pp. 1266–1274, 2004.

[6] J. N. Juang and R. S. Pappa, "An eigensystem realization algorithm for modal parameter identification and model reduction," *Journal of Guidance, Control, and Dynamics*, vol. 8, no. 5, pp. 620–627, 1985.

[7] D. E. Raveh, "Reduced-order models for nonlinear unsteady aerodynamics," *AIAA Journal*, vol. 39, no. 8, pp. 1417–1429, 2001.

[8] T. J. Cowan, A. S. Arena, and K. K. Gupta, "Accelerating computational fluid dynamics based aeroelastic predictions using system identification," *Journal of Aircraft*, vol. 38, no. 1, pp. 81–87, 2001.

[9] A. Mannarino and P. Mantegazza, "Nonlinear aerodynamic reduced order modeling by discrete time recurrent neural networks," *Aerospace Science and Technology*, vol. 47, pp. 406–419, 2015.

[10] F. D. Marques and J. Anderson, "Identification and prediction of unsteady transonic aerodynamic loads by multi-layer functionals," *Journal of Fluids and Structures*, vol. 15, no. 1, pp. 83–106, 2001.

[11] W. Zhang, B. Wang, Z. Ye, and J. Quan, "Efficient method for limit cycle flutter analysis based on nonlinear aerodynamic reduced-order models," *AIAA Journal*, vol. 50, no. 5, pp. 1019–1028, 2012.

[12] T. J. Mackman, C. B. Allen, M. Ghoreyshi, and K. J. Badcock, "Comparison of adaptive sampling methods for generation of surrogate aerodynamic models," *AIAA Journal*, vol. 51, no. 4, pp. 797–808, 2013.

[13] R. Huang, H. Hu, and Y. Zhao, "Nonlinear reduced-order modeling for multiple-input/multiple-output aerodynamic systems," *AIAA Journal*, vol. 52, no. 6, pp. 1219–1231, 2014.

[14] B. Glaz, L. Liu, and P. P. Friedmann, "Reduced-order nonlinear unsteady aerodynamic modeling using a surrogate-based recurrence framework," *AIAA Journal*, vol. 48, no. 10, pp. 2418–2429, 2010.

[15] D. Amsallem, J. Cortial, and C. Farhat, "Towards real-time computational-fluid-dynamics-based aeroelastic computations using a database of reduced-order information," *AIAA Journal*, vol. 48, no. 9, pp. 2029–2037, 2010.

[16] T. Skujins and C. Cesnik, "Toward an unsteady aerodynamic ROM for multiple Mach regimes," in *53rd AIAA/ASME/ASCE/AHS/ASC Structures, Structural Dynamics and Materials Conference*, Honolulu, Hawaii, April 2012.

[17] M. Ghoreyshi, R. M. Cummings, A. D. Ronch, and K. J. Badcock, "Transonic aerodynamic load modeling of X-31 aircraft pitching motions," *AIAA Journal*, vol. 51, no. 10, pp. 2447–2464, 2013.

[18] H. Liu, H. Hu, Y. Zhao, and R. Huang, "Efficient reduced-order modeling of unsteady aerodynamics robust to flight parameter variations," *Journal of Fluids and Structures*, vol. 49, pp. 728–741, 2014.

[19] M. Winter and C. Breitsamter, "Neurofuzzy-model-based unsteady aerodynamic computations across varying free-stream conditions," *AIAA Journal*, vol. 54, no. 9, pp. 2705–2720, 2016.

[20] H. Liu, R. Huang, Y. Zhao, and H. Hu, "Reduced-order modeling of unsteady aerodynamics for an elastic wing with control surfaces," *Journal of Aerospace Engineering*, vol. 30, no. 3, pp. 1–19, 2016.

[21] T. W. Simpson, J. D. Poplinski, P. N. Koch, and J. K. Allen, "Metamodels for computer-based engineering design: survey and recommendations," *Engineering with Computers*, vol. 17, no. 2, pp. 129–150, 2001.

[22] N. V. Queipo, R. T. Haftka, W. Shyy, T. Goel, R. Vaidyanathan, and P. Kevin Tucker, "Surrogate-based analysis and optimization," *Progress in Aerospace Sciences*, vol. 41, no. 1, pp. 1–28, 2005.

[23] P. Van Overschee and B. De Moor, *Subspace Identification for Linear Systems: Theory, Implementation, Applications*, Kluwer Academic, Dordrecht, the Netherlands, 1996.

[24] S. S. Davis, "NACA64A010 oscillatory pitching. Compendium of unsteady aerodynamics measurements," *AGARD Report-702*, 1982.